Comparing first-principles density functionals plus corrections for the lattice dynamics of $YBa_2Cu_3O_6$

Jinliang Ning,[1] Christopher Lane,[2] Bernardo Barbiellini,[3,4] Robert S. Markiewicz,[4] Arun Bansil,[4] Adrienn Ruzsinszky,[1, a)] John P. Perdew,[1, b)] and Jianwei Sun[1, c)]

[1)] *Department of Physics and Engineering Physics, Tulane University, New Orleans, Louisiana 70118, United States*

[2)] *Theoretical Division, Los Alamos National Laboratory, Los Alamos, New Mexico 87545, USA*

[3)] *Department of Physics, School of Engineering Science, LUT University, FI-53851 Lappeenranta, Finland*

[4)] *Department of Physics, Northeastern University, Boston, MA 02115, USA*

(Dated: 18 December 2023)

The enigmatic mechanism underlying unconventional high-temperature superconductivity, especially the role of lattice dynamics, has remained a subject of debate. Theoretical insights have long been hindered due to the lack of an accurate first-principles description of the lattice dynamics of cuprates. Recently, using the r2SCAN meta-GGA functional, we were able to achieve accurate phonon spectra of an insulating cuprate $YBa_2Cu_3O_6$, and discover significant magnetoelastic coupling in experimentally interesting Cu-O bond stretching optical modes [Phys. Rev. B 107, 045126 (2023)]. We extend this work by comparing PBE and r2SCAN performances with corrections from the on-site Hubbard U and the D4 van der Waals (vdW) methods, aiming at further understanding on both the materials science side and the density functional side. We demonstrate the importance of vdW and self-interaction corrections for accurate first-principles $YBa_2Cu_3O_6$ lattice dynamics. Since r2SCAN by itself partially accounts for these effects, the good performance of r2SCAN is now more fully explained. In addition, the performances of the Tao-Mo series of meta-GGAs, which are constructed in a different way from SCAN/r2SCAN, are also compared and discussed.

I. INTRODUCTION

Despite the decades of vigorous efforts devoted to the understanding of unconventional high-temperature superconductivity in the cuprates, a consensus on the underlying mechanism has yet to be reached[1–6]. Early theoretical works[7–9] suggested that the conventional BCS theory (electron-phonon coupling mechanism)[10–12] could not account for such high critical temperatures in cuprate superconductors. However, a more intricate and intriguing picture has been suggested by recent experimental findings[13–19]. Strong anomalies in Cu-O bond-stretching modes are found near optimal doping, which is associated with charge inhomogeneity and beyond previous pictures and understandings[14]. Optical spectroscopy results indicate that the electron-phonon coupling contributes at least 10% of the bosonic pairing glue, although antiferromagnetic spin fluctuations are deemed as the main mediators[20]. Moreover, the electronic interactions and the electron-phonon coupling are found to reinforce each other in a positive-feedback loop, which in turn enhances superconductivity, as suggested by recent ARPES observations[19].

Part of the reason why the role of phonons was dismissed by the theoretical community was that previous density functional theory (DFT) calculations at the local density approximation (LDA) and generalized gradient approximation (GGA) levels failed to find strong electron-phonon coupling in related cuprates[8]. This issue is related to and compounded by the fact that these density functional approximations (DFAs) cannot stabilize the correct electronic and magnetic ground state in the parent phase, let alone its evolution with doping[21,22]. While corrections such as the Hubbard U[23–26] method can stabilize the antiferromagnetic (AFM) ground state[27], their structural predictions can be unexpected and uncontrollable[28]. Obviously, an *ab initio* treatment is required to capture simultaneously the electronic, magnetic and lattice degrees of freedom.

Recently, utilizing the r2SCAN meta-GGA functional[29], some of us[30] were able to stabilize the AFM state of the pristine oxide $YBa_2Cu_3O_6$, and faithfully reproduce the experimental phonon dispersions. We further found significant magnetoelastic coupling in numerous high-energy Cu-O bond stretching optical branches, where the AFM results improve over the soft nonmagnetic phonon bands[30]. Moreover, these phonons correspond to breathing modes within the CuO_2 plane, suggesting a sensitive dependence on magnetoelastic coupling, which may facilitate a positive-feedback loop between electronic, magnetic, and lattice degrees of freedom. The r2SCAN functional is a modified and improved version of the strongly-constrained and appropriately-normed (SCAN) meta-GGA functional[31,32], which satisfies 17 exact constraints, and has demonstrated excellent performance across a diverse range of bonding environments. For

[a)] Electronic mail: aruzsin@tulane.edu
[b)] Electronic mail: perdew@tulane.edu
[c)] Electronic mail: jsun@tulane.edu

cuprates, SCAN accurately predicts the correct half-filled AFM ground state and the observed insulator-metal transition upon doping[21,22]. Moreover, SCAN provides improved estimates of lattice constants, across correlated and transition metal compounds[21,22,31–38]. Thus, SCAN is promising in accurate descriptions of lattice dynamics of cuprates and associated electron-phonon couplings, by virtue of its ability to capture the electronic and magnetic ground states. Unfortunately, reliable phonon spectra from SCAN calculations can be challenging due to numerical instability problems, although it could still be reachable with extra computational cost[39,40] or more advanced phonon calculation techniques[41–43]. By design, r2SCAN[29] solves the numerical instability problem and delivers accurate, transferable, and reliable lattice dynamics for various systems with different bonding characteristics[39]. We thus chose r2SCAN instead of SCAN for the study of lattice dynamics of $YBa_2Cu_3O_6$ and achieved remarkable success.

Despite this success, there still exists a notable residual softening trend in the Cu-O bond-stretching optical phonon branches from r2SCAN, especially in the full-breathing modes, for which we achieved further improvements when a Hubbard U correction is applied to r2SCAN[30]. Note that similar improvements from DFT+U were reported for optical modes of La_2CuO_4[27] and Mott insulator UO_2[44]. Furthermore, it is not fully understood why r2SCAN/SCAN perform so well on cuprates. Although in general we can attribute it to the power of satisfying exact constraints by design in SCAN/r2SCAN[29,31,45,46], more specific and physical knowledge will be helpful and highly required. Previous studies suggest that vdW corrections are important for first-principles prediction of lattice constants and cohesive energy of ionic solids and heavy metals[47]. In addition, combining vdW correction and self-interaction correction (SIC) is of critical importance for ground state electronic, structural and energetic properties of transition metal monoxides[36]. Therefore, it is expected that the vdW correction and its combination with SIC are crucial for obtaining accurate phonon dispersions of cuprates based on DFT.

To confirm this, in this work we extend our lattice dynamics study of $YBa_2Cu_3O_6$ by comparing the PBE and r2SCAN performances with corrections from the Hubbard U (applied to the *d* orbitals of Cu) and the D4 van der Waals (vdW) correction methods[48–51], aiming at further understanding both the physics of cuprate lattice dynamics and density functionals. We demonstrate the importance of vdW interactions and SIC for $YBa_2Cu_3O_6$ lattice dynamics. Since r2SCAN by itself provides a partial account of these effects to a greater degree than PBE, the better performance of r2SCAN is more fully explained. In addition, the performances of the Tao-Mo family of meta-GGAs (TMs)[52–54] are also compared and discussed. The original Tao-Mo meta-GGA (TM)[52] is constructed based on a density matrix expansion of the exchange hole model, while revTM[53] and rregTM[54] are two successors with modifications. The revTM includes a correlation correction obtained from the full high-density second-order gradient expansion, while rregTM includes a regulation to the order-of-limit problem[55], paired with a one-electron self-interaction-free correlation energy functional. In comparison, SCAN and r2SCAN are constructed by satisfying exact-constraints on the exchange-correlation energy[29,31,45,46]. Due to the inherently different way the Tao-Mo meta-GGAs are constructed compared to SCAN/r2SCAN, a comparison of their performances will be interesting and is expected to shed light on both the materials science side in cuprate lattice dynamics and the DFT side. Due to the absence of D4 parametrizations matched to TM functionals, the effects of vdW corrections to TMs are not considered in this work.

The synergy of long-range vdW corrections and +U SIC that we find here for cuprate lattice dynamics has also been found[36] for structural properties and structural phase transitions in MnO, FeO, CoO, and NiO.

II. METHODS

First-princiles calculations were performed using the pseudopotential projector-augmented wave method[56,57] with the Vienna *ab initio* simulation package (VASP)[58,59] with an energy cutoff of 600 eV for the plane-wave basis set. Several exchange-correlation functionals including PBE at the GGA level, and r2SCAN[29,39], TM[52], revTM[53], and rregTM[54] at the meta-GGA level were used. For the D4 vdW correction, we use the literature parametrizations fitted separately for PBE (s_6=1.0000, s_8=0.9595, a_1=0.3857, a_2=4.8069)[50] and for r2SCAN (s_6=1.0000, s_8=0.6019, a_1=0.5156, a_2=5.7734)[51]. A Gamma-centered 8×8×4 mesh for the **k**-space sampling is used for the relaxation of the unit cell with a G-type AFM structure, while a 2×2×2 mesh is used for the 2×2×1 supercells for force constant calculations of the phonon dispersion. The Fermi smearing method (ISMEAR = -1) was used, set with a low electronic temperature (SIGMA = 0.002 eV). All atomic sites in the unit cell along with the cell dimensions were relaxed using a conjugate gradient algorithm to minimize the energy with an atomic force tolerance of 0.001 eV/Å and a total energy tolerance of 10^{-7} eV. The harmonic force constants were extracted from VASP using the finite displacement method (0.015Å) as implemented in the Phonopy code[60].

III. RESULTS

Table I compares various properties calculated from various methods to available experimental values for $YBa_2Cu_3O_6$. The bare DFA results are compared with those with Hubbard U or/and vdW corrections. For the bare DFAs considered here, they all overestimate the lattice constants and underestimate the magnetic moments,

TABLE I. Calculated lattice constants, volume, Cu magnetic moment, Cu-O plane buckling angle ∠O-Cu-O, and Cu-O bond lengths for $YBa_2Cu_3O_6$ in the G-type AFM phase, along with the available experimental data. The Cu-O bond length for the two adjacent Cu-O planes in the *ab* plane, where Cu shows local magnetic moment m, is denoted by $d_{\mathrm{Cu-O}}$, while $z_{\mathrm{Cu-O_{ap}}}$ (nonmagnetic Cu-apical O bond) and $z'_{\mathrm{Cu-O_{ap}}}$ (magnetic Cu-apical O bond) denote the Cu-O bond lengths along the c direction. For PBE and r2SCAN, the Hubbard U and vdW (D4 and rVV10) corrections are considered. The choice of Hubbard U values is guided by both experimental lattice constants and Cu magnetic moment.

DFA	U	vdW	a (Å)	c (Å)	V (Å^3)	m (μ_B)	$d_{\mathrm{Cu-O}}$ (Å)	∠O-Cu-O (°)	$z_{\mathrm{Cu-O_{ap}}}$ (Å)	$z'_{\mathrm{Cu-O_{ap}}}$ (Å)
PBE	0	–	3.8819	12.1905	183.70	0.00	1.948	170.32	1.816	2.672
	6	–	3.8750	12.0379	180.76	0.59	1.950	167.06	1.811	2.551
	6	D4	3.8525	11.8702	176.17	0.59	1.938	167.25	1.803	2.492
r2SCAN	0	–	3.8570	11.9417	177.65	0.45	1.937	169.28	1.805	2.554
	5	–	3.8562	11.8321	175.95	0.66	1.941	167.00	1.795	2.472
	4	D4	3.8485	11.8032	174.82	0.62	1.936	167.41	1.794	2.469
	4	rVV10	3.8482	11.7638	174.21	0.62	1.936	167.41	1.793	2.451
TM	0	–	3.8651	11.8224	176.61	0.15 (0.3)	1.939	170.31	1.812	2.502
	5	–	3.8626	11.7186	174.84	0.62	1.943	167.56	1.803	2.421
revTM	0	–	3.8649	11.8952	177.68	0.09 (0.3)	1.940	170.09	1.810	2.535
	5	–	3.8621	11.7919	175.89	0.61	1.943	167.52	1.802	2.451
rregTM	0	–	3.8982	11.9688	181.88	0.39	1.956	170.17	1.832	2.548
	5	–	3.8941	11.8648	179.92	0.63	1.960	166.74	1.824	2.445
Expt.			3.8544[a]	11.8175[a]	175.57[a]	0.55[b]	1.940	166.78	1.786	2.471

[a] Powder neutron diffraction at temperature of 5 K[61].
[b] Single crystal neutron scattering[62].

in different d egrees. In particular, PBE overestimates the lattice constants the most and at the same time is not able to stabilize the correct G-type AFM ground state, while r2SCAN and the TMs at the meta-GGA level can stabilize the G-type AFM ground state, and improve over PBE for structural properties. In addition, notable difference can be observed in the performances of these different meta-GGAs. TM gives the closest structural properties but notably underestimates the magnetic moments. The revTM functional performs similarly with TM in structural properties but worse in magnetic moments. The rregTM functional improves in magnetic moments but worsens in structural properties. The r2SCAN functional in general predicts a good combination of structural and magnetic properties. What's more, TM and revTM predict different m agnetic m oments f or t he G-type AFM unit cell and the 2×2×1 supercells used for interatomic force constants calculations. This suggests that they could stabilize some spin-density-wave states rather than the simple G-type AFM ground state, which can be confirmed to some extent by the imaginary frequencies in the calculated phonon dispersions as shown in Fig. 4. The large spurious imaginary bands from TMs or/and their U-corrected versions also indicate that they may suffer much more serious numerical instability problems compared even to SCAN.

Applying a Hubbard U correction to these DFAs will reduce the delocalization error and increase the predicted magnetic moments. At the same time it also improves the structural properties, which will not be true for LSDA+U as we found previously since LSDA already underestimates the lattice constants[30]. In general, due to self-interaction reduction, the meta-GGAs require smaller U corrections than PBE[64]. The structural properties can be further improved with additional vdW corrections, as demonstrated by the PBE+U+D4 and r2SCAN+U+D4 results. Similarly to SCAN, r2SCAN captures intermediate range vdW interactions[32] while PBE captures little[65]. Therefore, more vdW correction is needed for PBE than r2SCAN, and correspondingly the structural improvements from the vdW correction are greater when applied to PBE than to r2SCAN. As a comparison and cross-check, almost the same structural and magnetic results are achieved with r2SCAN+rVV10[40] and r2SCAN+D4[51]. Note that the difference in the predicted lattice constant c from the two vdW corrections is more noticeable. Unfortunately, we are not sure which one is more reliable at the current stage. For the current calculated lattice constants, the zero-point energy effect is not considered. So, only some qualitative trend can be claimed, rather than quantitative comparisons especially when the difference is very small. It is possible that rVV10 is more accurate than D4, but the U value in r2SCAN+U+D4 or r2SCAN+U+rVV10 is too large, given that the resulting magnetic moment is larger than the experimental one. It is also possible that the b parameter in r2SCAN+rVV10 fitted from the Ar dimer binding curve is overbinding solid systems where the screening effect is usually stronger than that in molecules, as confirmed to some extent by the case of PBE+rVV10L[65] where a larger b (less vdW correction) is found to work better for layered materials. The current finding of the importance of vdW corrections to property predictions of $YBa_2Cu_3O_6$ is consistent with previous reports that vdW corrections are important for structural and energetic properties of ionic solids[47],

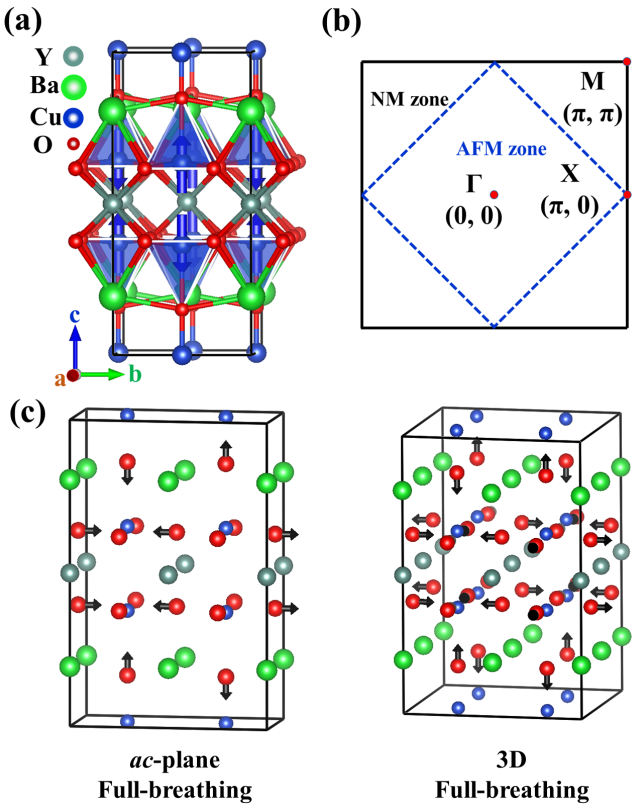

FIG. 1. (a) $\sqrt{2} \times \sqrt{2} \times 1$ crystal structure of $YBa_2Cu_3O_6$ where the related G-type AFM structure is highlighted by coloring the corner-sharing Cu-O pyramids blue(orange) for spin up(down). (b) A schematic of the nonmagnetic (black dashed line) and G-type AFM (blue dashed line) Brillouin zones and high-symmetry **k**-points. (c) Schematic of the typical *ac*-plane and 3D full-breathing modes.

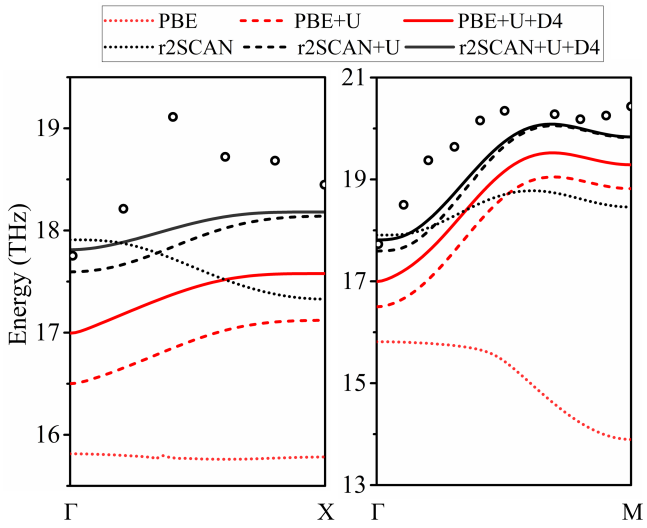

FIG. 2. Comparison of the *ac*-plane full-breathing branch (highest branch of Δ1) and the 3D full-breathing branch (highest branch of Σ1) for $YBa_2Cu_3O_6$, calculated from PBE, PBE+U (6 eV), PBE+D4+U (6 eV), r2SCAN, r2SCAN+U (5 eV) and r2SCAN+D4+U (4 eV) methods, with the experimental data (open circles)[63]. The Brillouin zone and high-symmetry **k**-points are shown in Fig. 1. The phonon results are obtained with supercell interatomic forces calculated with the same DFA (+U+D4) methods as for geometry relaxations, as detailed in Table I.

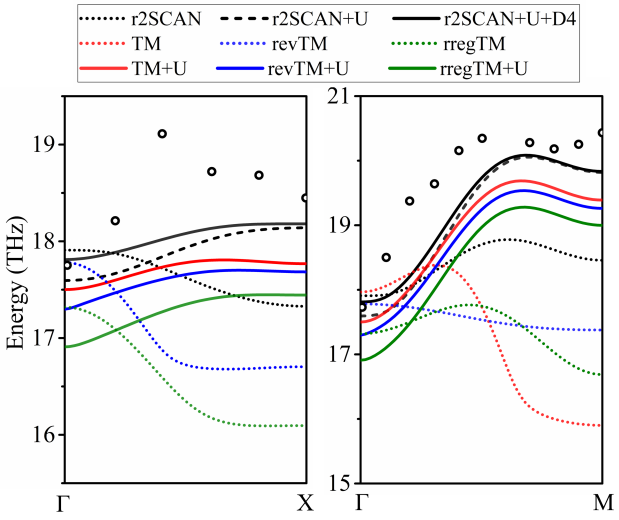

FIG. 3. Same as Fig. 2, but calculated results are from TM, TM+U (5 eV), revTM, revTM+U (5 eV), rregTM, rregTM+U (5 eV), r2SCAN, r2SCAN+U (5 eV), and r2SCAN+D4+U (4 eV) methods. Due to the complicated band crossing, the bare TM results are not shown for the *ac*-plane full-breathing branch.

and that the combination of vdW and Hubbard U corrections are important for the ground state electronic, structural and energetic properties of transition metal monoxides[36]. It is also consistent with the underestimation of lattice constants in LSDA, since LSDA tends to overbind weak bonds. Generally speaking, the improvements of meta-GGAs over GGAs can be attributed to the power of satisfying more exact constraints[45,46], but additionally the self-interaction reduction and better capture of vdW interactions at least contribute to a major part of their improvements. In addition, for PBE and r2SCAN, although applying larger Hubbard U alone can yield structural properties closer to experiment, it could over-localize *d* electrons and predict too large magnetic moments, highlighting the different physics of the two corrections and the necessity of appropriately applying both together. Since the phonon dispersion is determined by the inter-atomic forces, which depend sensitively on the ground state electronic structure and equilibrium atomic positions, the improvements for structural and electronic/magnetic properties from vdW and Hubbard U corrections bode well for more accurate predictions of the lattice dynamics.

The phonon dispersion results for the most challenging and also experimentally most interesting *ac*-plane and three-dimensional (3D) full-breathing branches, as shown

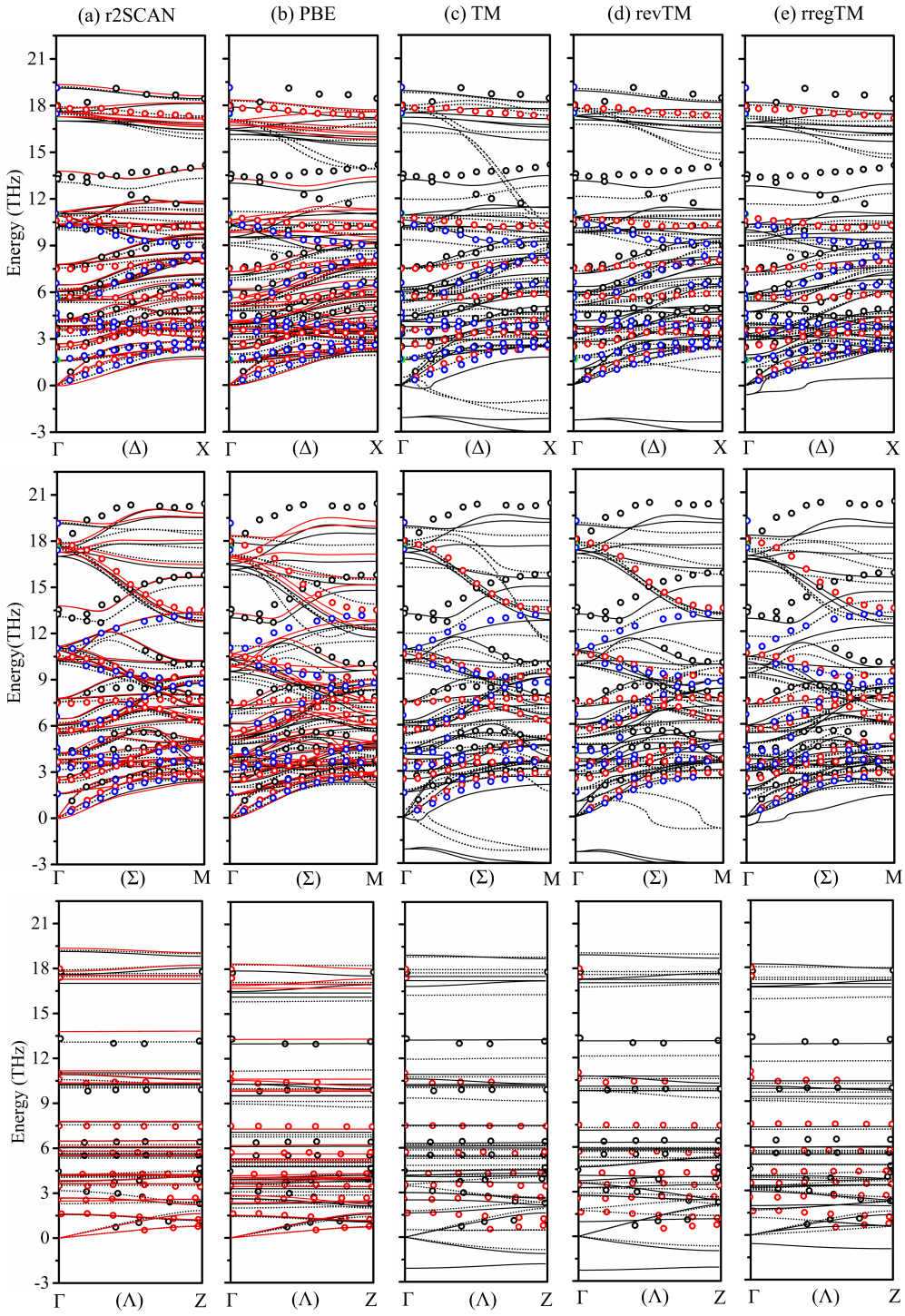

FIG. 4. Comparison of full plots of the phonon dispersions of $YBa_2Cu_3O_6$ including experimental data[63] (circles) and calculated results from DFAs and corrections based on (a) r2SCAN, (b) PBE, (c) TM, (d) revTM, and (e) rregTM. The bare DFA, DFA+U, and DFA+U+D4 results are represented as blacked dotted, black solid, and red solid lines,respectively. The U values applied are the same as in Figs. 2 and 3.

in Fig. 2 and Fig. 3, confirm our expectations. Both the *ac*-plane and 3D full-breathing modes involve the Cu-O bond-stretching vibrations within the Cu-O plane, and simultaneously the vibration of the apical oxygen in the *c* direction. The difference is that the *ab* Cu-O plane bond-stretching vibrations happen along both *a* and *b* directions for the 3D full-breathing modes, while only along either *a* or *b* direction for the *ac*-plane (or *bc*-plane) full-breathing modes, as shown in Fig. 1c. Figure 2 compares the bare PBE and r2SCAN results and those from Hubbard U and D4 vdW corrections. Both bare PBE and r2SCAN results are too soft for the two challenging branches, and the PBE results are even softer, similar to the previous nonmagnetic results from r2SCAN[30]. This is consistent with the fact that bare PBE cannot stabilize the AFM ground state and overestimates lattice constants. With U and vdW corrections, notable improvements are achieved for both PBE and r2SCAN, and the improvement is more significant for PBE than for r2SCAN, although the r2SCAN+U+D4 results remain closest to experiment. This is consistent with the observations and reasons discussed above for the structural and magnetic properties. To summarize, due to self-interaction reduction and capture of more intermediate range vdW interactions, r2SCAN performs much better than PBE in magnetic, structural and lattice dynamics properties of $YBa_2Cu_3O_6$, and for that reason the improvements from vdW and Hubbard U corrections are more significant for PBE than r2SCAN.

Figure 3 includes the bare TMs and Hubbard U corrected results, compared with r2SCAN+U+D4 and experimental results. All the bare TMs results are too soft compared to those from r2SCAN, consistent with the fact that r2SCAN gives the best bare DFA predictions in basic magnetic and structural properties which is critical for accurate lattice dynamics predictions. With Hubbard U correction, the improvement is significant and the results are close to but still softer than the r2SCAN+U+D4 results. Therefore r2SCAN generally has better performance than TMs for $YBa_2Cu_3O_6$ in structural, magnetic and lattice dynamics properties. This could be attributed to the more nonlocal nature of r2SCAN compared to TMs, since nonlocality is important for descriptions of semiconductors and insulators. Although both are at the same meta-GGA level, r2SCAN is more α-dependent and thus displays more nonlocality, while the TMs are more density gradient-dependent and less fully-nonlocal. This argument of the significance of nonlocality is consistent with an interesting and effective model proposed by Falter et al.[66–68], which separates the roles of local and nonlocal charge responses in phonons of cuprates. Additionally, Fig. 4 shows the experimental and calculated phonon dispersions for all optical and acoustic modes. Note that there are soft acoustic modes for all the TM functionals, with imaginary frequencies signaling structural instabilities predicted by the TM functionals.

IV. CONCLUSIONS

In summary, we have extended our previous work to a first-principles comparative study of the most challenging and experimentally important full-breathing modes of $YBa_2Cu_3O_6$. We achieve further understanding of both the lattice dynamics side and the density functional side. By applying both Hubbard U and the D4 vdW corrections to PBE and r2SCAN, notable improvements are obtained for structural, electronic, magnetic, and phonon dispersion predictions of $YBa_2Cu_3O_6$. The improvements from the combined corrections are more significant for PBE than for r2SCAN. With the improvements, PBE+U+D4 gives much better full-breathing phonon frequencies, closer but still softer compared to those from r2SCAN+U+D4 and experimental observations. Considering the general self-interaction reduction and capture of more intermediate-range vdW in r2SCAN, in comparison with PBE, we demonstrate the importance of vdW interactions and SIC in accurate $YBa_2Cu_3O_6$ lattice dynamics from first-principles, which in turn contributes to the major reason for the superior overall performance of r2SCAN over PBE.

In addition, for the family of Tao-Mo meta-GGAs, all the bare DFA results are too soft compared to those from r2SCAN. With similar Hubbard U corrections, improvements are notable but still not enough to be as good as r2SCAN with corrections. Therefore r2SCAN generally has better performance than TMs for $YBa_2Cu_3O_6$ in structural, magnetic and lattice dynamics properties, which we attribute to the more nonlocal nature of r2SCAN compared to TMs. Nevertheless, the TMs could perform better[69] for doped or gapless systems such as $YBa_2Cu_3O_7$[9,21,70], as implied by their good performances in surface, vacancy, and magnetic properties for metals[53,71], which could be further studied in the future. Kaplan and Perdew[69] argued that the perfect long-range screening of the exact exchange hole by the exact correlation hole in a metal can be better captured by the semi-locality of PBE (and by extension of the TM functionals) than by the fully-nonlocal density dependence of SCAN and r2SCAN (or the stronger full non-locality of many hybrid functionals).

Note that, even with the best results we can achieve from r2SCAN+U+D4, there still exists noticeable softening for the tested full-breathing branches, especially for the peak at $\mathbf{k} \sim (0.2, 0, 0)$ along the experimental *ac*-plane full-breathing branch. These residual discrep-ancies could imply extra physics or effects we have not included yet, such as lattice anharmonicity, dynamical multiferroicity[72], hidden order beyond the simple antiferromagnetic ground state[73,74], and so on. Recent research efforts have renewed interest in the role of electron-phonon coupling in the mechanism of high-temperature superconductivity in cuprates[75]. The findings in the current work provide insights for future first-principles investigations on cuprates, including phonon anomalies[7–9], charge inhomogeneity, cavity-phonon-magnon quasipar-

ticle interactions[76], and phase competition, which in turn contribute to a better understanding of cuprate high temperature superconducting materials.

ACKNOWLEDGMENTS

J.N. and J.S. acknowledge the support of the U.S. Office o f N aval R esearch (ONR) G rant N o. N00014-22-1-2673, with which they designed the project. J.N., A.R. and J.P.P acknowledge support from Tulane University's startup funds (computations). J.P.P. acknowledges support from the National Science Foundation under Grant. No. DMR-1939528. Computational work done at Tulane University was supported by the Cypress Computational Cluster at Tulane and the National Energy Research Scientific Computing Center. The work at Northeastern University was supported by the US Department of Energy (DOE), Office of Science, Basic Energy Sciences Grant No. DE-SC0022216 (accurate modeling of complex materials) and benefited from Northeastern University's Advanced Scientific Computation Center and the Discovery Cluster and the National Energy Research Scientific Computing Center through DOE Grant No. DE-AC02-05CH11231. The work at Los Alamos National Laboratory was supported by the U.S. DOE NNSA under Contract No. 89233218CNA000001 and by the Center for Integrated Nanotechnologies, a DOE BES user facility, in partnership with the LANL Institutional Computing Program for computational resources. Additional support was provided by DOE Office of Basic Energy Sciences Program E3B5. B.B. was supported by the Ministry of Education and Culture (Finland) and by the LUT University INERCOM platform.

DATA AVAILABILITY STATEMENT

The data that support the findings o f t his s tudy are available from the corresponding author upon reasonable request.

[1] J. G. Bednorz and K. A. Müller, "Possible high T_C superconductivity in the Ba-La-Cu-O system," Zeitschrift für Physik B Condensed Matter **64**, 189–193 (1986).
[2] P. W. Anderson, "The resonating valence bond state in La_2CuO_4 and superconductivity," Science **235**, 1196–1198 (1987).
[3] C. C. Tsuei and J. R. Kirtley, "Pairing symmetry in cuprate superconductors," Rev. Mod. Phys. **72**, 969–1016 (2000).
[4] A. Damascelli, Z. Hussain, and Z.-X. Shen, "Angle-resolved photoemission studies of the cuprate superconductors," Rev. Mod. Phys. **75**, 473–541 (2003).
[5] B. Keimer, S. A. Kivelson, M. R. Norman, S. Uchida, and J. Zaanen, "From quantum matter to high-temperature superconductivity in copper oxides," Nature **518**, 179–186 (2015).
[6] J. A. Sobota, Y. He, and Z.-X. Shen, "Angle-resolved photoemission studies of quantum materials," Rev. Mod. Phys. **93**, 025006 (2021).
[7] K.-P. Bohnen, R. Heid, and M. Krauss, "Phonon dispersion and electron-phonon interaction for $YBa_2Cu_3O_7$ from first-principles calculations," EPL (Europhysics Letters) **64**, 104 (2003).
[8] F. Giustino, M. L. Cohen, and S. G. Louie, "Small phonon contribution to the photoemission kink in the copper oxide superconductors," Nature **452**, 975–978 (2008).
[9] R. Heid, R. Zeyher, D. Manske, and K.-P. Bohnen, "Phonon-induced pairing interaction in $YBa_2Cu_3O_7$ within the local-density approximation," Phys. Rev. B **80**, 024507 (2009).
[10] L. N. Cooper, "Bound electron pairs in a degenerate fermi gas," Phys. Rev. **104**, 1189–1190 (1956).
[11] J. Bardeen, L. N. Cooper, and J. R. Schrieffer, "Microscopic theory of superconductivity," Phys. Rev. **106**, 162–164 (1957).
[12] J. Bardeen, L. N. Cooper, and J. R. Schrieffer, "Theory of superconductivity," Phys. Rev. **108**, 1175–1204 (1957).
[13] R. J. McQueeney, J. L. Sarrao, P. G. Pagliuso, P. W. Stephens, and R. Osborn, "Mixed lattice and electronic states in high-temperature superconductors," Phys. Rev. Lett. **87**, 077001 (2001).
[14] D. Reznik, L. Pintschovius, M. Ito, S. Iikubo, M. Sato, H. Goka, M. Fujita, K. Yamada, G. Gu, and J. Tranquada, "Electron-phonon coupling reflecting dynamic charge inhomogeneity in copper oxide superconductors," Nature **440**, 1170–1173 (2006).
[15] A. Lanzara, P. Bogdanov, X. Zhou, S. Kellar, D. Feng, E. Lu, T. Yoshida, H. Eisaki, A. Fujimori, K. Kishio, *et al.*, "Evidence for ubiquitous strong electron-phonon coupling in high-temperature superconductors," Nature **412**, 510–514 (2001).
[16] M. d'Astuto, P. K. Mang, P. Giura, A. Shukla, P. Ghigna, A. Mirone, M. Braden, M. Greven, M. Krisch, and F. Sette, "Anomalous dispersion of longitudinal optical phonons in $Nd_{1.86}Ce_{0.14}CuO_{4+\delta}$ determined by inelastic x-ray scattering," Phys. Rev. Lett. **88**, 167002 (2002).
[17] R. J. McQueeney, Y. Petrov, T. Egami, M. Yethiraj, G. Shirane, and Y. Endoh, "Anomalous dispersion of LO phonons in $La_{1.85}Sr_{0.15}CuO_4$ at low temperatures," Phys. Rev. Lett. **82**, 628–631 (1999).
[18] G.-H. Gweon, T. Sasagawa, S. Zhou, J. Graf, H. Takagi, D.-H. Lee, and A. Lanzara, "An unusual isotope effect in a high-transition-temperature superconductor," Nature **430**, 187–190 (2004).
[19] Y. He, M. Hashimoto, D. Song, S.-D. Chen, J. He, I. Vishik, B. Moritz, D.-H. Lee, N. Nagaosa, J. Zaanen, *et al.*, "Rapid change of superconductivity and electron-phonon coupling through critical doping in Bi-2212," Science **362**, 62–65 (2018).
[20] S. Dal Conte, C. Giannetti, G. Coslovich, F. Cilento, D. Bossini, T. Abebaw, F. Banfi, G. Ferrini, H. Eisaki, M. Greven, *et al.*, "Disentangling the electronic and phononic glue in a high-T_C superconductor," Science **335**, 1600–1603 (2012).
[21] Y. Zhang, C. Lane, J. W. Furness, B. Barbiellini, J. P. Perdew, R. S. Markiewicz, A. Bansil, and J. Sun, "Competing stripe and magnetic phases in the cuprates from first principles," Proceedings of the National Academy of Sciences **117**, 68–72 (2020).
[22] J. W. Furness, Y. Zhang, C. Lane, I. G. Buda, B. Barbiellini, R. S. Markiewicz, A. Bansil, and J. Sun, "An accurate first-principles treatment of doping-dependent electronic structure of high-temperature cuprate superconductors," Communications Physics **1**, 1–6 (2018).
[23] V. I. Anisimov, J. Zaanen, and O. K. Andersen, "Band theory and Mott insulators: Hubbard U instead of Stoner I," Phys. Rev. B **44**, 943–954 (1991).
[24] M. Cococcioni and S. de Gironcoli, "Linear response approach to the calculation of the effective interaction parameters in the LDA + U method," Phys. Rev. B **71**, 035105 (2005).
[25] D. Kasinathan, J. Kune**s**, K. Koepernik, C. V. Diaconu, R. L. Martin, I. m. c. D. Prodan, G. E. Scuseria, N. Spaldin, L. Petit, T. C. Schulthess, and W. E. Pickett, "Mott transition of mno under pressure: A comparison of correlated band theories," Phys. Rev. B **74**, 195110 (2006).
[26] S. L. Dudarev, G. A. Botton, S. Y. Savrasov, C. J. Humphreys, and A. P. Sutton, "Electron-energy-loss spectra and the structural stability of nickel oxide: An LSDA+U study," Phys. Rev. B **57**, 1505–1509 (1998).

[27] T. C. Sterling and D. Reznik, "Effect of the electronic charge gap on LO bond-stretching phonons in undoped La_2CuO_4 calculated using LDA+U," Physical Review B **104**, 134311 (2021).

[28] T. Jarlborg, B. Barbiellini, C. Lane, Y. J. Wang, R. Markiewicz, Z. Liu, Z. Hussain, and A. Bansil, "Electronic structure and excitations in oxygen deficient $CeO_{2-\delta}$ from DFT calculations," Physical Review B **89**, 165101 (2014).

[29] J. W. Furness, A. D. Kaplan, J. Ning, J. P. Perdew, and J. Sun, "Accurate and numerically efficient r2SCAN meta-generalized gradient approximation," J. Phys. Chem. Lett. **11**, 8208–8215 (2020).

[30] J. Ning, C. Lane, Y. Zhang, M. Matzelle, B. Singh, B. Barbiellini, R. S. Markiewicz, A. Bansil, and J. Sun, "Critical role of magnetic moments in the lattice dynamics of $yba_2cu_3o_6$," Phys. Rev. B **107**, 045126 (2023).

[31] J. Sun, A. Ruzsinszky, and J. P. Perdew, "Strongly constrained and appropriately normed semilocal density functional," Phys. Rev. Lett. **115**, 036402 (2015).

[32] J. Sun, R. C. Remsing, Y. Zhang, Z. Sun, A. Ruzsinszky, H. Peng, Z. Yang, A. Paul, U. Waghmare, X. Wu, *et al.*, "Accurate first-principles structures and energies of diversely bonded systems from an efficient density functional," Nature chemistry **8**, 831 (2016).

[33] Y. Zhang, J. Furness, R. Zhang, Z. Wang, A. Zunger, and J. Sun, "Symmetry-breaking polymorphous descriptions for correlated materials without interelectronic U," Phys. Rev. B **102**, 045112 (2020).

[34] Y. Zhang, J. W. Furness, B. Xiao, and J. Sun, "Subtlety of TiO_2 phase stability: Reliability of the density functional theory predictions and persistence of the self-interaction error," The Journal of Chemical Physics **150**, 014105 (2019).

[35] D. A. Kitchaev, H. Peng, Y. Liu, J. Sun, J. P. Perdew, and G. Ceder, "Energetics of MnO_2 polymorphs in density functional theory," Phys. Rev. B **93**, 045132 (2016).

[36] H. Peng and J. P. Perdew, "Synergy of van der waals and self-interaction corrections in transition metal monoxides," Phys. Rev. B **96**, 100101 (2017).

[37] J. Ning, Y. Zhu, J. Kidd, Y. Guan, Y. Wang, Z. Mao, and J. Sun, "Subtle metastability of the layered magnetic topological insulator $MnBi_2Te_4$ from weak interactions," npj Computational Materials **6**, 1–6 (2020).

[38] C. Lane, Y. Zhang, J. W. Furness, R. S. Markiewicz, B. Barbiellini, J. Sun, and A. Bansil, "First-principles calculation of spin and orbital contributions to magnetically ordered moments in Sr_2IrO_4," Phys. Rev. B **101**, 155110 (2020).

[39] J. Ning, J. W. Furness, and J. Sun, "Reliable lattice dynamics from an efficient density functional approximation," Chemistry of Materials **34**, 2562–2568 (2022).

[40] J. Ning, M. Kothakonda, J. W. Furness, A. D. Kaplan, S. Ehlert, J. G. Brandenburg, J. P. Perdew, and J. Sun, "Workhorse minimally empirical dispersion-corrected density functional with tests for weakly bound systems: r2scan+rvv10," Phys. Rev. B **106**, 075422 (2022).

[41] M. A. Mathis, A. Khanolkar, L. Fu, M. S. Bryan, C. A. Dennett, K. Rickert, J. M. Mann, B. Winn, D. L. Abernathy, M. E. Manley, D. H. Hurley, and C. A. Marianetti, "Generalized quasiharmonic approximation via space group irreducible derivatives," Phys. Rev. B **106**, 014314 (2022).

[42] E. Xiao, H. Ma, M. S. Bryan, L. Fu, J. M. Mann, B. Winn, D. L. Abernathy, R. P. Hermann, A. R. Khanolkar, C. A. Dennett, D. H. Hurley, M. E. Manley, and C. A. Marianetti, "Validating first-principles phonon lifetimes via inelastic neutron scattering," Phys. Rev. B **106**, 144310 (2022).

[43] S. Bandi and C. A. Marianetti, "Precisely computing phonons via irreducible derivatives," Phys. Rev. B **107**, 174302 (2023).

[44] S. Zhou, H. Ma, E. Xiao, K. Gofryk, C. Jiang, M. E. Manley, D. H. Hurley, and C. A. Marianetti, "Capturing the ground state of uranium dioxide from first principles: Crystal distortion, magnetic structure, and phonons," Phys. Rev. B **106**, 125134 (2022).

[45] J. W. Furness, A. D. Kaplan, J. Ning, J. P. Perdew, and J. Sun, "Construction of meta-GGA functionals through restoration of exact constraint adherence to regularized SCAN functionals," The Journal of Chemical Physics **156**, 034109 (2022).

[46] A. D. Kaplan, M. Levy, and J. P. Perdew, "The predictive power of exact constraints and appropriate norms in density functional theory," Annual Review of Physical Chemistry **74**, 193–218 (2023).

[47] J. Tao, F. Zheng, J. Gebhardt, J. P. Perdew, and A. M. Rappe, "Screened van der waals correction to density functional theory for solids," Phys. Rev. Mater. **1**, 020802 (2017).

[48] E. Caldeweyher, C. Bannwarth, and S. Grimme, "Extension of the D3 dispersion coefficient model," The Journal of Chemical Physics **147**, 034112 (2017).

[49] E. Caldeweyher, J.-M. Mewes, S. Ehlert, and S. Grimme, "Extension and evaluation of the d4 london-dispersion model for periodic systems," Physical Chemistry Chemical Physics **22**, 8499–8512 (2020).

[50] E. Caldeweyher, S. Ehlert, A. Hansen, H. Neugebauer, S. Spicher, C. Bannwarth, and S. Grimme, "A generally applicable atomic-charge dependent London dispersion correction," The Journal of Chemical Physics **150**, 154122 (2019).

[51] S. Ehlert, U. Huniar, J. Ning, J. W. Furness, J. Sun, A. D. Kaplan, J. P. Perdew, and J. G. Brandenburg, "r2SCAN-D4: Dispersion corrected meta-generalized gradient approximation for general chemical applications," The Journal of Chemical Physics **154**, 061101 (2021).

[52] J. Tao and Y. Mo, "Accurate semilocal density functional for condensed-matter physics and quantum chemistry," Phys. Rev. Lett. **117**, 073001 (2016).

[53] S. Jana, K. Sharma, and P. Samal, "Improving the performance of tao-mo non-empirical density functional with broader applicability in quantum chemistry and materials science," The Journal of Physical Chemistry A **123**, 6356–6369 (2019).

[54] S. Jana, S. K. Behera, S. Śmiga, L. A. Constantin, and P. Samal, "Accurate density functional made more versatile," The Journal of Chemical Physics **155** (2021).

[55] J. W. Furness, N. Sengupta, J. Ning, A. Ruzsinszky, and J. Sun, "Examining the order-of-limits problem and lattice constant performance of the Tao-Mo functional," The Journal of Chemical Physics **152**, 244112 (2020).

[56] P. E. Blöchl, "Projector augmented-wave method," Phys. Rev. B **50**, 17953–17979 (1994).

[57] G. Kresse and D. Joubert, "From ultrasoft pseudopotentials to the projector augmented-wave method," Phys. Rev. B **59**, 1758 (1999).

[58] G. Kresse and J. Furthmüller, "Efficient iterative schemes for ab initio total-energy calculations using a plane-wave basis set," Phys. Rev. B **54**, 11169–11186 (1996).

[59] G. Kresse and J. Hafner, "Ab initio molecular dynamics for open-shell transition metals," Physical Review B **48**, 13115 (1993).

[60] A. Togo and I. Tanaka, "First principles phonon calculations in materials science," Scripta Materialia **108**, 1–5 (2015).

[61] R. Cava, A. Hewat, E. Hewat, B. Batlogg, M. Marezio, K. Rabe, J. Krajewski, W. Peck Jr, and L. Rupp Jr, "Structural anomalies, oxygen ordering and superconductivity in oxygen deficient $Ba_2YCu_3O_x$," Physica C: Superconductivity **165**, 419–433 (1990).

[62] H. Casalta, P. Schleger, E. Brecht, W. Montfrooij, N. H. Andersen, B. Lebech, W. W. Schmahl, H. Fuess, R. Liang, W. N. Hardy, and T. Wolf, "Absence of a second antiferromagnetic transition in pure $YBa_2Cu_3O_{6+x}$," Phys. Rev. B **50**, 9688–9691 (1994).

[63] S. Chaplot, W. Reichardt, L. Pintschovius, and N. Pyka, "Common interatomic potential model for the lattice dynamics of several cuprates," Physical Review B **52**, 7230 (1995).

[64] R. B. Wexler, G. S. Gautam, and E. A. Carter, "Exchange-correlation functional challenges in modeling quaternary chalcogenides," Phys. Rev. B **102**, 054101 (2020).

[65]H. Peng and J. P. Perdew, "Rehabilitation of the perdew-burke-ernzerhof generalized gradient approximation for layered materials," Phys. Rev. B **95**, 081105 (2017).
[66]C. Falter, M. Klenner, and W. Ludwig, "Effect of charge fluctuations on the phonon dispersion and electron-phonon interaction in la_2cuo_4," Phys. Rev. B **47**, 5390–5404 (1993).
[67]C. Falter, M. Klenner, G. A. Hoffmann, and F. Schnetgöke, "Dipole polarization and charge transfer effects in the lattice dynamics and dielectric properties of ionic crystals," Phys. Rev. B **60**, 12051–12060 (1999).
[68]C. Falter, "Phonons, electronic charge response and electron–phonon interaction in the high-temperature superconductors," physica status solidi (b) **242**, 78–117 (2005).
[69]A. D. Kaplan and J. P. Perdew, "Laplacian-level meta-generalized gradient approximation for solid and liquid metals," Phys. Rev. Mater. **6**, 083803 (2022).
[70]L. Pintschovius, D. Reznik, W. Reichardt, Y. Endoh, H. Hiraka, J. M. Tranquada, H. Uchiyama, T. Masui, and S. Tajima, "Oxygen phonon branches in $YBa_2Cu_3O_7$," Phys. Rev. B **69**, 214506 (2004).
[71]S. Jana, A. Patra, and P. Samal, "Assessing the performance of the Tao-Mo semilocal density functional in the projector-augmented-wave method," The Journal of Chemical Physics **149**, 044120 (2018).
[72]D. M. Juraschek, M. Fechner, A. V. Balatsky, and N. A. Spaldin, "Dynamical multiferroicity," Phys. Rev. Mater. **1**, 014401 (2017).
[73]A. de la Torre, K. Seyler, L. Zhao, S. Di Matteo, M. Scheurer, Y. Li, B. Yu, M. Greven, S. Sachdev, M. Norman, *et al.*, "Mirror symmetry breaking in a model insulating cuprate," Nature Physics **17**, 777–781 (2021).
[74]A. de la Torre, S. Di Matteo, D. Hsieh, and M. Norman, "Implications of second harmonic generation for hidden order in sr 2 cuo 2 cl 2," Physical Review B **104**, 035138 (2021).
[75]I. Ahmadova, T. C. Sterling, A. C. Sokolik, D. L. Abernathy, M. Greven, and D. Reznik, "Phonon spectrum of underdoped $HgBa_2CuO_{4+\delta}$ investigated by neutron scattering," Phys. Rev. B **101**, 184508 (2020).
[76]J. B. Curtis, A. Grankin, N. R. Poniatowski, V. M. Galitski, P. Narang, and E. Demler, "Cavity magnon-polaritons in cuprate parent compounds," Phys. Rev. Research **4**, 013101 (2022).